Journal of Electroanalytical Chemistry 855 (2019) 113495

Contents lists available at ScienceDirect

Journal of Electroanalytical Chemistry

journal homepage: www.elsevier.com/locate/jelechem

Gold nanoparticles decorated on single layer graphene applied for electrochemical ultrasensitive glucose biosensor

Yawen Yuan [a], Yishi Wang [b], Hua Wang [a,*], Shifeng Hou [a]

[a] National Engineering and Technology Research Center for Colloidal Materials, Shandong University, Jinan, Shandong, 250100, PR China
[b] Institute 53 of China North Industries Group Corporation, Jinan, Shandong, 250031, PR China

ARTICLE INFO

Keywords:
Chemical vapor deposition
Monolayer graphene
Sputtering
Electrochemical
Perspiration-based glucose biosensor

ABSTRACT

A glucose biosensor was fabricated by glucose oxidase (GOD) immobilized on gold nanoparticles decorated on single layer graphene (Au/SLG) modified glassy carbon electrode, with 6-(ferrocenyl)hexanethiol (Fc–C_6H_{12}–SH) as electron transfer medium (GOD/Fc/Au/SLG/GCE). The free-standing Au/SLG was obtained by sputtered gold nanoparticles on chemical vapor deposition (CVD)-generated monolayer graphene. This process avoids complicated polymer-transfer processes of graphene and affords AuNPs with good dispersion and clean surface promoting immobilization of GOD. Since the clean surface and lower background current of free-polymer-transferred CVD-generated graphene, the ductility monolayer graphene is suit for ultrasensitive detection of low concentration of glucose. Synergy with electron mediator facilitates electron transfer process, the sensor has enhanced electrochemical performance with the detection limit of 0.1 nM (S/N = 3) and good selectivity. The sensor was further studied for real perspiration test with attractive feasibility, which has potential application in perspiration-based wearable glucose detection.

1. Introduction

Sensitive detection of glucose has been widely studied for the value in diabetes diagnosis field [1–3]. Electrochemical methods were widely investigated, including invasive, minimally invasive, and non-invasive detection in skin interstitial fluid and biofluids [4–9]. Among them, non-invasive glucose detection addresses the limitations of finger-stick blood testing, represents the ideal choice for advanced diabetes management in perspiration, salivary and tears samples [10,11]. Especially, sensitivity sensor was developed to detect lower concentration of glucose in perspiration samples, which diffusing from blood vessels with a correlation of 10 μM to 0.7 mM in diabetic patients [12,13]. In addition, analysis of practical perspiration samples can be applied in the field of flexible wearable non-invasive glucose detection and therapeutic drug delivery in the future [14,15].

Glucose oxidase (GOD) was widely used to fabricate glucose biosensor cause its sensitivity and specificity for glucose detection [16]. Gold nanoparticle has larger surface-to-volume ratio and outstanding conductivity, what's more, it is stable, modifiability, and biocompatibility than other metal nanoparticals, which was widely used as immobilizer agents and electrode modifiers [17]. Graphene, as the thinnest two-dimensional carbon material with large specific surface area, remarkable mechanical and electrical properties, was also widely used due to the advantages of increasing loading capacity and improve electron transport [18–21]. All them together, gold nanoparticles decorated graphene immobilized GOD modified electrode, was expect to accurately measure ultralow concentration of glucose, especially in perspiration samples [22–26].

Specially, graphene as an important support material has an elevated space for optimizing the detection performance of the sensor. Graphene powder have the residual of oxygen-containing functional groups and surfactants induced from synthesized process, which reducing the electrical conductivity and leading insensitive detection. Interlayer agglomeration of graphene also reduces surface area and exposure of the active site of the supported catalyst [27–29]. The Chemical vapor deposition (CVD) method is cracking carbon source into carbon atoms at higher temperature, then depositing or segregating them on growth substrate at lower temperature. CVD-generated graphene can be single layer with good crystal quality, avoid layer stacking and inducing oxygen-containing functional groups. It is superior to construct more sensitive sensor because it maintains excellent electrical conductivity and good ductility [30,31]. However, the complicated transfer process by polymethyl methacrylate (PMMA) or polydimethylsiloxane (PDMS) adhering to the surface of graphene and etching the growth substrate

* Corresponding author.
E-mail address: h.wang@sdu.edu.cn (H. Wang).

https://doi.org/10.1016/j.jelechem.2019.113495
Received 29 November 2018; Received in revised form 15 September 2019; Accepted 16 September 2019
Available online 1 November 2019

could remain polymer on surface of graphene, which lead to insensitive detection [32].

Here, we use CVD-generated graphene bonded sputtering technology to prepare a self-supporting graphene/gold nanoparticles composite film without polymer assist transfer, which is used to immobilize GOD for ultralow concentration glucose detection. Sputtering deposited gold nanoparticles avoid residual surfactant; single layer graphene prepared by CVD can achieve good dispersion and active surface area maximum exposure of gold nanoparticles, which were beneficial to the immobilization of the enzyme. 6-(ferrocenyl)hexanethiol (Fc–C_6H_{12}–SH) as electron transfer mediators was used to realize the electron transfer between redox enzyme center and electrode surface [33–35]. Sputtered gold nanoparticles as medium were used to attach 6-(ferrocenyl)hexanethiol and 6-amino-1-hexanethiol hydrochloride to electrode by forming Au–S bonds. The glutaraldehyde was used as crosslinking agent in order to attached GOD to the modified electrode through connecting aldehyde groups (–CHO) with amino groups (–NH_2) of GOD and 6-amino-1-hexanethiol hydrochloride by Schiff base reaction. The optimized biosensor towards glucose ultralow concentration detection was evaluated by cyclic voltammetry (CV), differential pulse voltammetry (DPV) and electrochemical impedance spectroscopy (EIS) models.

2. Experimental

2.1. Reagents and apparatus

Copper foils with 25 μm thick and 99.8% purity were bought from Alfa Aesar Company. Hydrogen (H_2), methane (CH_4) and nitrogen (N_2) gases with 99.99% purity were bought from Jinan Deyang Special gas Company. The reduced graphene oxide (RGO) dispersion in water (1 mg/mL) was purchased from Leadernano Tech. L.L.C. Glucose oxidase (GOD, from aspergillus niger, ≥15,000 units/g solid, without added oxygen), 6-(ferrocenyl)hexanethiol and 6-amino-1-hexanethiol hydrochloride were both bought from Sigma-Aldrich Co. L.L.C. Glutaraldehyde (24–26% mass fraction in water) was obtained from J&K Scientific Ltd. Glucose ($C_6H_{12}O_6$), ammonium persulfate ($(NH_4)_2S_2O_8$), disodium hydrogen phosphate dihydrate ($Na_2HPO_4{\cdot}2H_2O$) and sodium dihydrogen phosphate dihydrate ($NaH_2PO_4{\cdot}2H_2O$) were procured from Sinopharm Chemical Regent Company. Glassy carbon electrode and gold electrode were polished with aluminum oxide powders with diameters of 50 nm and 300 nm, purchased from Shanghai Chenhua Instrument Company. The phosphate buffered solution (pH = 7) was prepared by $Na_2HPO_4{\cdot}2H_2O$ and $NaH_2PO_4{\cdot}2H_2O$ with concentration of 0.1 mol L^{-1}. Glucose oxidase (GOD) solution (5 mg/mL) was prepared by GOD powder dissolved in phosphate buffered solution (0.1 mol L^{-1}, pH = 7) and stored in 4 °C refrigerator. All reagents in experiments were of analytical grade and used as received. All water used in experiments were ultrapure water with a resistivity of 18.2 MΩcm.

Single layer graphene was obtained by G-CVD equipment from Xicheng Company. The vacuum sputter equipment was obtained from Denton Vacuum Company (DESK V Cold Sputter, Moorestown, USA). The 99.999% purity gold target was bought from GRIKIN Advanced Material Company. All electrochemistry measurements were carried out in the electrochemical workstation (CHI–660C) bought from Shanghai Chen-Hua Instrument Company. Electrochemical studies were performed using a standard three-electrode system. Platinum (Pt) plate was used as the counter electrode and saturated calomel electrode (SCE) used as the reference electrode, respectively. A glassy carbon electrode (GCE) with diameters of 3 mm was polished to mirror finish using Al_2O_3 suspension and sonicated in ultrapure water and ethanol in sequence. The cleaned GCE was used to attach to Au/SLG in the solution ensuring the graphene was contact with GCE and the gold nanoparticles were exposed outside of the electrode. The modified electrode was dried overnight in air so that the graphene was in stable contact with the electrode.

All transmission electron microscopy (TEM) images were taken by JEM-1011 (JEOL). Scanning electron microscopy (SEM) images were performed by JSM-6700F. The structure and feature of materials were analyzed by Raman spectroscopy (PHS–3C) and X-ray photoelectron spectroscopy (ThermoFisher K-Alpha).

2.2. Preparation of Au/SLG/GCE and GOD/Fc/Au/SLG/GCE

2.2.1. Au/SLG/GCE

Chemical vapor deposition single layer graphene support gold nanoparticles modified glassy carbon electrode, was prepared as our previous report, which denoted as Au/SLG/GCE [36]. Briefly, the gold nanoparticles were sputtered on the typical low-pressure chemical vapor deposition (LPCVD) graphene growth on copper foils, with the sputtering power output of 30 W and sputtering time of 30 s. Then copper foil with growth graphene was etching by 0.2 mol/L $(NH_4)_2S_2O_8$ for one night and washed several times by water. The free-standing gold nanoparticles decorated graphene (Au/SLG) film was float on water finally. Glassy carbon electrode (GCE) picked up the Au/SLG films to ensure that graphene adhered the surface of GCE and gold nanoparticles are exposed to the outside. Then modified electrode was dried in nature and short as Au/SLG/GCE.

2.2.2. GOD/Fc/Au/SLG/GCE

The 6-(ferrocenyl)hexanethiol and GOD modified Au/SLG/GCE, short for GOD/Fc/Au/SLG/GCE was prepared as working electrode. First of all, the Au/SLG/GCE was immersed in the mixed solution of 6-(ferrocenyl) hexanethiol and 6-amino-1-hexanethiol hydrochloride (2 mmol/L) for 4 h. Then, the modified electrode was dried in air and following immersed in glutaraldehyde solution for 4 h. Lastly, GOD solution (3 μL, 5 mg/mL) was dropped on the modified electrode. The modified electrode was stored in the 4 °C refrigerator overnight standby, abbreviated as GOD/Fc/Au/SLG/GCE.

2.3. Preparation of contrast electrodes

2.3.1. SLG/GCE

The single layer graphene on GCE was construct as SLG/GCE for comparison. In detail, PMMA solution (5 μL, 5% mass fraction) was spin coated on the surface of CVD-generated graphene on copper foils and cured at 120 °C for 2 h. Copper foils were etched by $(NH_4)_2S_2O_8$ solution (0.2 mol/L) overnight and the free-standing PMMA supported graphene film was suspended on the solution. Then the PMMA supported graphene film was transfer to the surface of GCE, the PMMA was removed by hot acetone. The monolayer graphene modified gold electrode was obtained, as short for SLG/GCE.

2.3.2. Fc/Au/SLG/GCE

The prepared modified electrode (Au/SLG/GCE) was immersed in 6-(ferrocenyl)hexanethiol solution (2 mmol/L) to link the sulfhydryl groups (–SH) with gold nanoparticles to form Au–S bonding. After soaking for 4 h, the obtained modified electrode was dried and denoted as Fc/Au/SLG/GCE.

2.3.3. GOD/Au/SLG/GCE

The GOD modified Au/SLG/GCE, short for GOD/Au/SLG/GCE was prepared as working electrode. First of all, the Au/SLG/GCE was immersed in the 6-amino-1-hexanethiol hydrochloride solution (2 mmol/L) for 4 h. Then, the modified electrode was dried in air and following immersed in glutaraldehyde solution for 4 h. Lastly, GOD solution (3 μL, 5 mg/mL) was dropped on the modified electrode. The modified electrode was stored in the 4 °C refrigerator overnight standby, abbreviated as GOD/Au/SLG/GCE.

2.3.4. Fc/GOD/Au/RGO/GCE

By replacing single layer CVD-grown graphene film with reduced graphene oxide (RGO) powder, the modified electrode Fc/GOD/Au/RGO/GCE was constructed. The RGO ethanol dispersion (5 μL, 1 mg mL^{-1}) was dropped on the removable GCE, then sputtering gold nanoparticals on

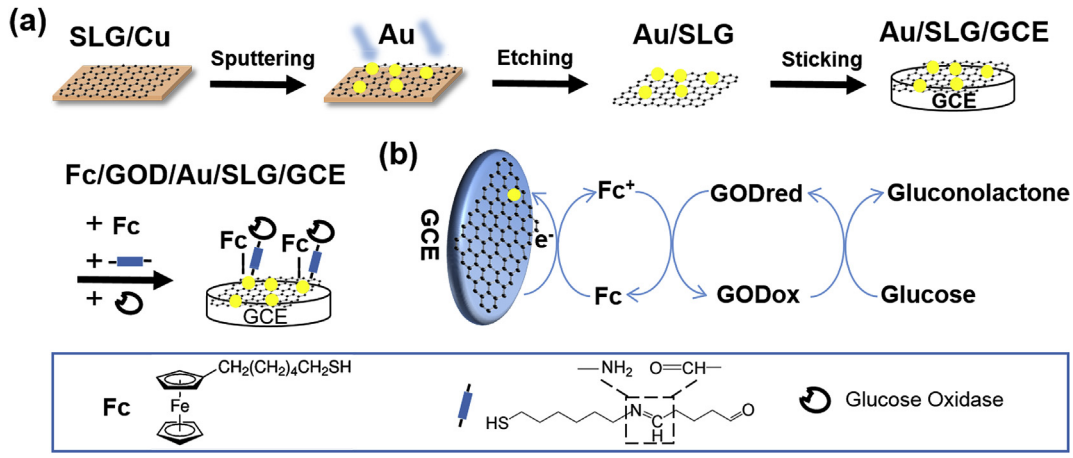

Scheme 1. (a) Process of synthesize GOD/Fc/Au/SLG/GCE, (b) GOD/Fc/Au/SLG/GCE application in glucose detection.

RGO/GCE, which obtain Au/RGO/GCE instead of Au/SLG/GCE. The other process is same as above to modify Fc and GOD, to obtain Fc/GOD/Au/RGO/GCE. That is, 6-(ferrocenyl)hexanethiol and GOD modified with RGO powder support gold nanoparticles on glassy carbon electrode was denoted as contrast electrode Fc/GOD/Au/RGO/GCE.

2.4. Electrochemical measurements

The electrochemical measurements were carried out using home-made electrolytic cell at room temperature, containing a beaker and cover plate with three electrodes insert. The 20 mL phosphate buffered solution (0.1 mol L^{-1}, pH = 7) were added in the beaker and bubbling with N_2 for 30 min to expel O_2. All working potentials were reported against the saturated calomel electrode (SCE).

The electrochemical behavior of modified electrodes was evaluated by cyclic voltammetry (CV), differential pulse voltammetry (DPV) and amperometric i-t curve models. The CV curves were recorded from - 0.1 V to 0.7 V (*vs.* SCE) to exhibit the electrochemical behavior of modified electrodes. The DPV model was used to measure the electrochemical response of different concentrations of glucose injected into phosphate buffered solution, ranging from −0.1 V to 0.7 V (*vs.* SCE). The amperometric i-t curve was recorded the anti-interference performance of biosensor, with 10 times glucose concentration of ascorbic acid (AA), uric acid (UA) and dopamine (DA) inject at 0.5 V (*vs*. SCE). The real sample analysis was also carried out in human perspiration samples.

3. Results and discussion

3.1. Principle

Scheme 1 is the preparation process of GOD/Fc/Au/SLG/GCE, starting from CVD-generated graphene. The mechanism of glucose oxidation has been reported previously as the second-generation biosensor with ferrocenyl derivate as electron transfer medium facilitating the electron transfer process [37]. The possible mechanism of electron transfer process shows in Scheme 1 (b) and reactions show as followed:

$$\text{Glucose} + \text{GOD (ox)} \rightarrow \text{Gluconolactone} + \text{GOD (red)}$$

$$\text{GOD (red)} + 2Fc^{+} \rightarrow \text{GOD (ox)} + 2Fc + 2H^{+}$$

$$2Fc \rightarrow 2Fc^{+} + 2e^{-}$$

3.2. Characterization of Au/SLG

Fig. 1 represents SEM image of Au/SLG on the surface of GCE with the well-dispersed gold nanoparticles (white dots) loaded on graphene. The SEM images of CVD-generated graphene and Au/SLG both loaded on GCE were shown in Fig. S1A and Fig. S1B. The CVD-generated graphene showed good ductility covered on surface of GCE and had some wrinkles caused by impurities. The TEM image of Au/SLG with the well-dispersed gold nanoparticles (black dots) loaded on graphene was also shown in Fig. S1C. It was confirming well ductility CVD-generated graphene act as good platform to avoid gold nanoparticles agglomeration. The size distribution histogram of gold nanoparticles was inset Fig. S1C, showing the average size with 8 nm (n = 180). Fig. S1D and inset photos were Au/SLG covered on GCE and floated in solution.

Raman spectroscopy was used as nondestructive tool to analyze layer numbers and crystal structure of graphene. The typical features peaks of graphene grown on copper foils are the G and 2D bands as shown in Fig. 2. The sharp peaks of G and 2D bands at ~ 2645.9 cm^{-1} and ~ 1588.7 cm^{-1} indicate graphene has good crystalline quality. The intensity ratio of I_{2D}/I_G identifies the number of graphene is single layer. The weak intensity of D peak at ~1329.5 cm^{-1} reveals the primarily form of graphene is sp^2 hybridized carbon atoms with few structure defect [38, 39]. The Raman spectrum of SLG transfer to GCE was also showed in Fig. 2. The PMMA assist transfer method was used to transfer CVD-generated graphene to the surface of GCE, the transfer process increased the defect of graphene with the increased D peak and D + D' peak. The Raman spectrum of Au/SLG identifies increased D peak and full width at half maximum (FWHM) of G and 2D peaks, along with slight blue shift of G peak and decreased intensity of 2D peak. These changes induced by increased disorder can attribute to the deposition process of

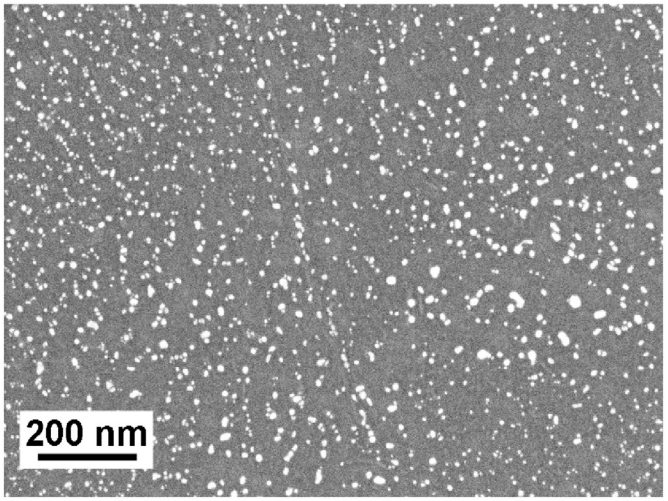

Fig. 1. SEM image of Au/SLG on GCE.

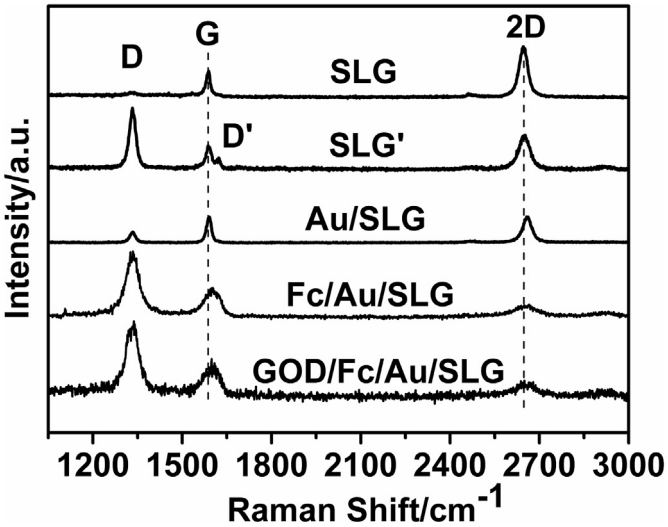

Fig. 2. Raman spectrums of single layer graphene on copper foil (SLG), single layer graphene transfer onto GCE (SLG′), Au/SLG, Fc/Au/SLG and GOD/Fc/Au/SLG on GCE.

the gold nanoparticles. The decreased intensity ratio of I_{2D}/I_G identifies the added number of graphene, which showed the tendency of graphene to form wrinkles. After 6-(ferrocenyl)hexanethiol (Fc–C_6H_{12}–SH) and GOD attached onto Au/SLG/GCE, the D peaks and full width at half maximum (FWHM) of G and 2D peaks increased obviously, which showed the increasing of defect structure.

Fig. 3 shows the C 1s and Au 4f XPS spectra of Au/SLG. The C 1s peak are fitted into three components associated with C═C, C–C and O–C═O, located at binding energies of 284.5 eV, 285.1 eV and 286.7 eV, respectively [40,41]. The C–C and C═C bonding assigned to sp^3 and sp^2 hybridized carbon atoms of graphene, and the weak oxidation of low intensity of O═C–O functional groups declaring the stability of graphene in the testing condition. The Au 4f peak are fitted into two components corresponding to Au(0) 4f 7/2 and Au(0) 4f 5/2, located at binding energies of 84.0 eV and 87.7 eV, respectively [42]. In addition, the present Au 4f peaks illustrates the sputtering process could deposit gold nanoparticles on graphene corresponding to others characterization.

3.3. Electrochemical response of modified electrodes

The electrochemical performance of contrast electrodes were studied using cyclic voltammogram (CV) model. The CV curves of glassy carbon electrode, GCE (a), single layer graphene on glassy carbon electrode, SLG/GCE (b), Au/SLG/GCE (c), Fc/Au/SLG/GCE (d) and GOD/Fc/Au/SLG/GCE (e) were shown in Fig. 4. In phosphate buffer solution, both

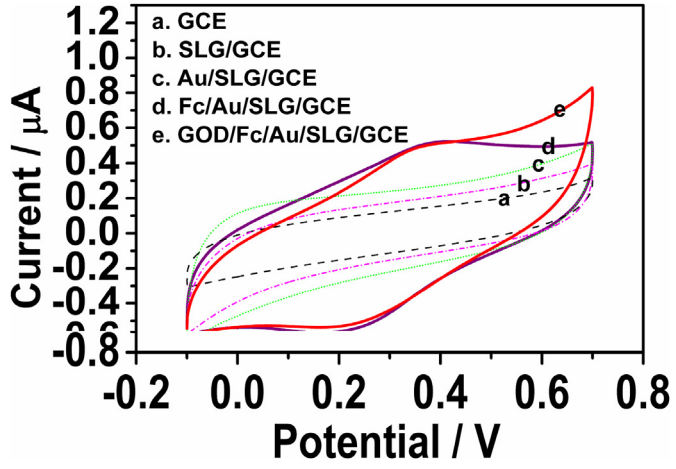

Fig. 4. Cyclic voltammogram curves of (a) glassy carbon electrode (GCE), (b) SLG/GCE, (c) Au/SLG/GCE, (d) Fc/Au/SLG/GCE and (e) GOD/Fc/Au/SLG/GCE in phosphate buffered solution with scan rate of 50 mV s^{-1}.

GCE, SLG/GCE and Au/SLG/GCE have no redox peak. The CV curves of Fc/Au/SLG/GCE and GOD/Fc/Au/SLG/GCE showed a pair of obvious redox peaks at 0.22 V and 0.37 V (*vs* SCE). The well-defined anodic and cathodic peaks were induced by the ferrocene moiety, indicating 6-(ferrocenyl)hexanethiol (Fc) was covalently bonded with Au/SLG/GCE for fast electron transfer.

The electrochemical behavior of GCE, Au/SLG/GCE and GOD/Fc/Au/SLG/GCE towards glucose oxidation was investigated as shown in Fig. 5(A). The GCE and Au/SLG/GCE have low capacitance in 20 mL phosphate buffered solution without glucose, and no redox peaks observed when 50 μM glucose injected into solution. It is revealing that GCE and Au/SLG are electrochemically silent for glucose in the potential range. By contrast, the CV curve of GOD/Fc/Au/SLG/GCE has obvious response peak at 0.55 V (*vs*. SCE) when 50 μM glucose added, corresponding to the conversion of GOD (ox) to GOD (red). In addition, cyclic voltammogram curves of Fc/Au/SLG/GCE and GOD/Au/SLG/GCE in phosphate buffered solution absent and present of 50 μM glucose were shown in Fig. S2. It can be seen that the lack of the electron mediator 6-(ferrocenyl)hexanethiol and glucose oxidase, the modified electrode cannot achieve detection of ultra-low concentration of glucose.

The investigation of different scan rate influenced the peak current value of GOD/Fc/Au/SLG/GCE present 50 μM glucose was performed in Fig. 5(B). The peak current values were increased with scan rate increased from 0.02 V/s to 0.2 V/s (inner to outer). The redox potentials were shifted slightly and the peak current values have well linearly relationship with scan rate. The linear relationships of peak current values with the scan rate were inset Fig. 5(B) with correlation coefficient of 0.998, indicating the adsorption dynamics control process. The

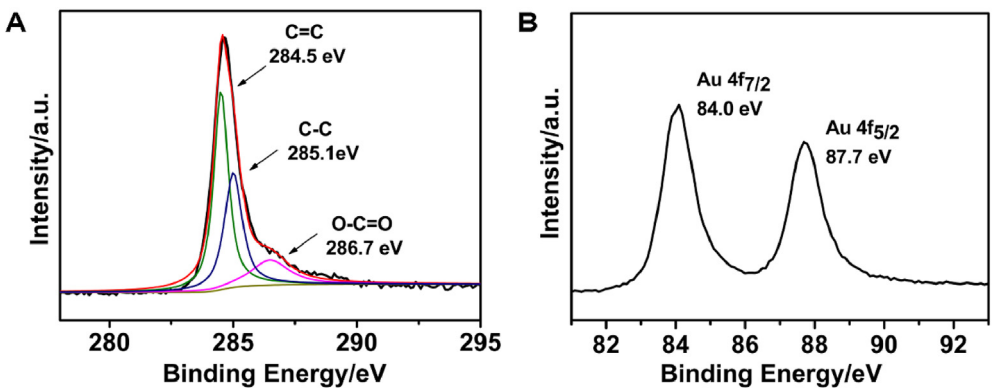

Fig. 3. XPS survey spectra of Au/SLG: (A) C 1s; (B) Au 4f.

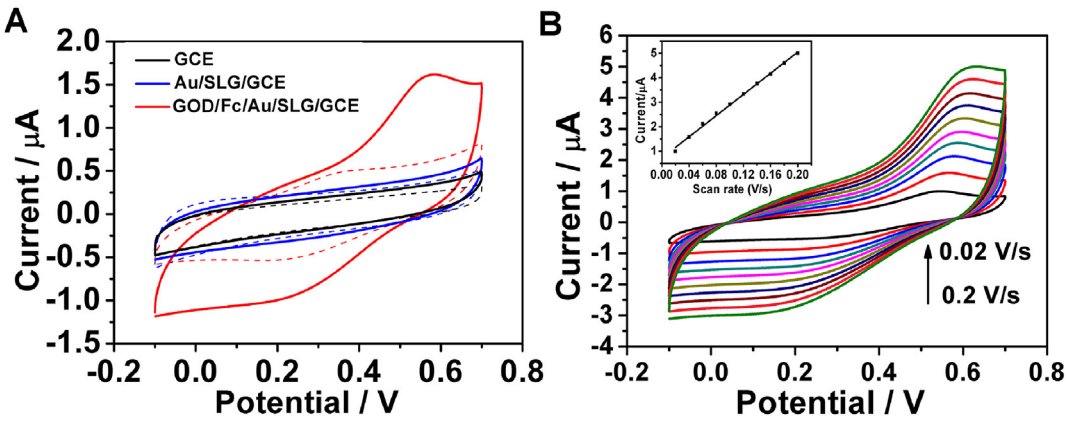

Fig. 5. (A) Cyclic voltammogram curves of GCE (black curve), Au/SLG/GCE (blue curve) and GOD/Fc/Au/SLG/GCE (red curve) in phosphate buffered solution absent (dash line) and present (solid line) of 50 μM glucose with scan rate of 50 mV s^{-1}; (B) cyclic voltammogram curves of GOD/Fc/Au/SLG/GCE in phosphate buffered solution containing 50 μM glucose at different scan rates from 0.02 V/s to 0.2 V/s with regular interval of 20 mV s^{-1}, inset was the plots of current value versus scan rate at 0.5 V (*vs.* SCE).

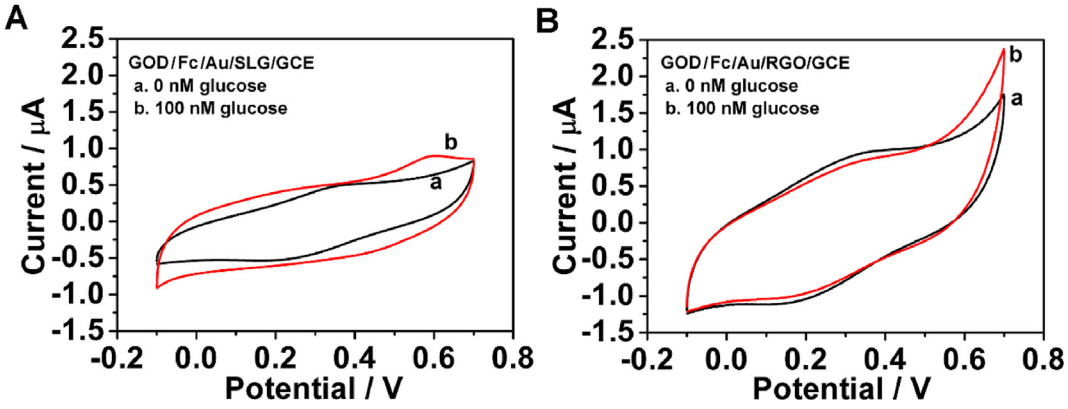

Fig. 6. Cyclic voltammogram curves of (A) GOD/Fc/Au/SLG/GCE and (B) GOD/Fc/Au/RGO/GCE in phosphate buffered solution (a curve) absent and (b curve) present 100 nM glucose with scan rate of 50 mV s^{-1}.

electron transfer properties of GCE, Au/SLG/GCE and GOD/Fc/Au/SLG/GCE were studied by CV and EIS techniques using standard ferricyanide solutions, as shown in Fig. S3.

The electrochemical behavior of GOD/Fc/Au/SLG/GCE and Fc/GOD/Au/RGO/GCE towards glucose oxidation was investigated as shown in Fig. 6(A) and Fig. 6(B) respectively. Both CV tests were carried out in 20 mL phosphate buffered solution with absent (a) and present (b) 100 nM glucose at the scan rate of 50 mV s^{-1} from −0.1 to 0.7 V (*vs.* SCE). The capacitance of GOD/Fc/Au/SLG/GCE is lower than Fc/GOD/Au/RGO/GCE in the phosphate buffered solution without glucose, which can account for the larger capacitance of RGO powder than CVD-generated single layer graphene [43]. Moreover, both of the modified electrodes have redox peak at 0.2 V and 0.35 V (*vs* SCE), account for the process of ferrocene moiety gain and loss electron. After added 100 nM glucose, the CV curve of GOD/Fc/Au/SLG/GCE ((b) curve in Fig. 6(A)) yielded a distinct peak at 0.58 V (*vs.* SCE). The redox peak indicates the

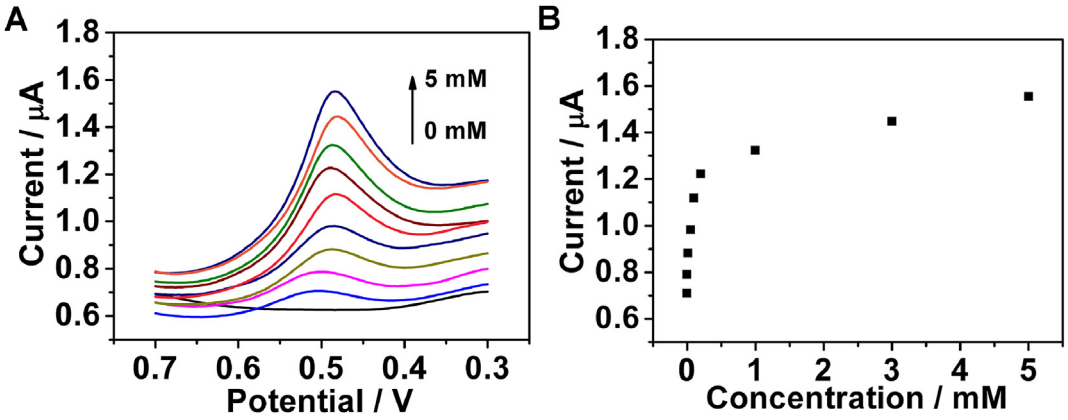

Fig. 7. (A) Differential pulse voltammetry curves of GOD/Fc/Au/SLG/GCE in phosphate buffered solution with different concentration of glucose from 0 nM, 1 nM, 0.1 μM, 10 μM, 50 μM, 100 μM, 200 μM, 1 mM, 3 mM and 5 mM; (B) the plots of current value versus concentration of glucose at 0.5 V (*vs.* SCE).

Table 1
Comparison of graphene-supported gold nanoparticles biosensor for glucose detection.

Materials	Linear range (μM)	Detection limit (μM)	Reference
GOx/PRGO-AuNPs[a]	0.4–4	0.06	[44]
GNS-PEI-AuNPs[b]	1–100	0.32	[45]
GA/GNs/GOD[c]	50–450	0.597	[46]
Nafion/GOD/f-G-Au[d]	~30,000	1	[47]
GOx/rGO/AuNR	10–7000	3	[48]
Graphene/AuNP/GOD/ Nafion	10–366	4	[49]
GA@GNs/GNs[e]	10–16000	4	[50]
GR-MWNTs/AuNPs/GOD	10–5200	4.1	[51]
Au/rGO/AuPtNP/GOx/ nafion	100–2300	5	[52]
PPy-RGO-(AuNPs-GOD)$_4$[f]	200–8000	5.6	[53]
Graphene-AuNPs-GOD	43.6–261.6	8.9	[54]
S-GNs-AuNPs-GOx[g]	1000–12000	9.3	[55]
GOD/AuNPs/graphene	0–2220	16.7	[56]
GOx/ERGO-AuNPs[h]	200–20000	17	[24]
AuNPs–rGO/GOD	2000–18000	45	[57]
GOx/AuNP/PANI/rGO/NH_2-MWCNTs[i]	1000–10000	64	[58]
GOx/graphene/PFLO/AuNPs[j]	100–1500	81	[59]
GOx/AuNPs-graphene-chitosan	2000–10000	180	[60]
SGN/Au/GOD[k]	2000–16000	200	[61]
GOx-GO–SH–Au	3000–9000	319.4	[62]
Fc/GOD/Au/SLG[l]	0.0005–5000	0.0001	This work

[a] PRGO: partially reduced graphene oxide.
[b] Glucose oxidase on graphene-polyethylenemine-gold nanoparticles hybrid.
[c] Graphene aerogel/gold nanoparticle/glucose oxidase.
[d] f-G-Au: functionalized graphene decorated with gold nanoparticles.
[e] Graphene aerogel-gold nanoparticles nanohybrids.
[f] Gold nanoparticles and glucose oxidase onto polypyrrole-reduced graphene oxide matrix.
[g] S-GNs: sulfur-modified graphene nanosheet.
[h] ERGO: electrochemical reduced graphene oxide.
[i] Glucose oxidase immobilized amine terminated multiwall carbon nanotubes/ reduced graphene oxide/polyaniline/gold nanoparticles.
[j] PFLO: poly(9,9-di-(2-ethylhexyl)-fluorenyl-2,7-diyl)-end capped with 2,5-diphenyl-1,2,4-oxadiazole.
[k] SGN: sulfonated graphene nanosheet.
[l] 6-(ferrocenyl)hexanethiol/glucose oxidase/gold nanoparticles/single layer graphene.

electrochemical oxidation of glucose, with 6-(ferrocenyl)hexanethiol as electron transfer intermediate and graphene as platform facilitate the electron transport process. The good response of GOD/Fc/Au/SLG/GCE towards low concentration of glucose detection can attribute to the low background current of SLG. In addition, the well exposure of gold nanoparticles to immobilize GOD enhanced catalytic efficiency. However, the Fc/GOD/Au/RGO/GCE ((b) curve in Fig. 6(B)) showed no obvious peaks towards glucose oxidation but a slight rise of current value.

3.4. DPV determination of glucose

The differential pulse voltammetry (DPV) model was used to measure the different concentrations of glucose injected into 20 mL phosphate buffered solution from 0.3 V to 0.7 V (*vs.* SCE) in Fig. 7(A). The concentration curves were 0 nM, 1 nM, 0.1 μM, 10 μM, 50 μM, 100 μM, 200 μM, 1 mM, 3 mM and 5 mM, respectively. The peak current values at 0.5 V were increased with increasing concentration of glucose. The current values mutated when higher concentrations of glucose were added, indicating the good sensitivity of the sensor toward ultralow concentrations of glucose. The linear correlation relationship of current with low and high concentration of glucose in Fig. 6(B) were $I = 0.7842 + 3.5234 \times C$ (μA, mM, $R^2 = 0.900$) and $I = 1.2341 + 0.06635 \times C$ (μA, mM, $R^2 = 0.970$), respectively. The detection range was ranged from 0.1 nM to 5 mM, with the detection limit of 0.1 nM at a signal-to-noise ratio of 3.

Table 1 has list similar graphene nanocomposites of glucose biosensors for comparison. The detection limit of the GOD/Fc/Au/SLG/GCE for glucose was lower to 0.1 nM (S/N = 3) than other similar materials. It can attribute to the residue-free and well-dispersed gold nanoparticles on graphene expose sites to attach GOD for better sensing performance. In addition, the low background current value and toughness of CVD-generated graphene is the key to ultra-low glucose sensitivity detection.

The selectivity of GOD/Fc/Au/SLG/GCE for glucose detection was examined by DPV curve as shown in Fig. S4. The interference species of 0.5 mM ascorbic acid (AA), uric acid (UA) and dopamine (DA) was injected into phosphate buffered solution containing 50 μM glucose. The current response curve shows the high selectivity of GOD/Fc/Au/SLG/GCE sensor for glucose detection.

3.5. Real sample detection

The feasibility of GOD/Fc/Au/SLG/GCE for practical applicability was further investigated with human perspiration samples by standard addition method. For actual sample determination experiments, filtered human sweat is used directly without additional treatment. The results listed in Table 2 demonstrated the good recovery percentage and yield of biosensor, which calculated from the current response curve in Fig. 7(B). The biosensor shows excellent capability to detect glucose in real perspiration samples with the acceptable relative standard deviations (RSD) of less than 5%. The successfully detection of ultralow concentration of glucose and practical analysis of perspiration samples confirmed the potential value in practical applications of perspiration-based biosensors.

3.6. Reproducibility, repeatability and stability study of biosensor

The reproducibility of biosensor was study by measuring response current value towards 0.5 mM glucose in N_2-saturated phosphate buffered solution (0.1 mol/L, pH = 7.0). The relative standard deviation (RSD) for 6 successive tests was 3.8%. In order to study the repeatability of the biosensor, three modified electrodes were prepared independently for the electrochemical determination of 0.5 mM glucose at different times. The results showed the average sensitivity and relative standard deviation of the biosensor were 6.8%. The biosensor was stored in a refrigerator at 4 °C. The stability of the biosensor was investigated by monitoring the current response of 0.5 mM glucose after two weeks, which retained 81% of the initial current response.

4. Conclusion

In this work, a glucose biosensor was fabricated via immobilization of glucose oxidase (GOD) and 6-(ferrocenyl)hexanethiol with gold

Table 2
Detection of glucose in human perspiration samples using GOD/Fc/Au/SLG/GCE (n = 3).

Samples	Spiked (μM)	Found (μM)	Recovery (%)	Added (μM)	Measured (μM)	Yield (%)	RSD (%)
1	10	10.98 ± 0.043	109.80	5	15.87 ± 0.018	117.40	3.14
2	50	48.75 ± 0.031	97.50	25	73.69 ± 0.061	94.76	2.75
3	100	101.58 ± 0.042	101.58	50	152.23 ± 0.034	104.46	2.48

RSD: relative standard deviation.

nanoparticles decorated single layer graphene modified GCE (GOD/Fc/Au/SLG/GCE). The free-standing CVD-generated graphene supported sputtering gold nanoparticles were successfully obtained by free polymer transfer method. The clean surface of gold nanoparticles with maximized exposure sites on large specific surface area of monolayer graphene were good for immobilizing glucose oxidase (GOD) and 6-(ferrocenyl)hexanethiol. In addition, the ferrocene derivatives were used as electron mediators to facilitate electrons transfer process.

The low background current of high quality single layer graphene supported gold nanoparticles account for the improved electrochemical performance even for ultralow concentrations detecting. The sensor has lower detection limit of 0.1 nM (S/N = 3) and wider detection range of 0.1 nM–5 mM. In addition, the sensor has good stability, anti-interference capability and good performance for real perspiration samples, which has huge potential value in flexibility perspiration-based wearable biosensors for real-time detection.

Acknowledgements

The National Natural Science Foundation of China (Grant No. 21475076) and International S&T collaboration Program of China (No. 2015DFA50060) financially supported this work.

Appendix A. Supplementary data

Supplementary data to this article can be found online at https://doi.org/10.1016/j.jelechem.2019.113495.

References

[1] Y. Eun-Hyung, L. Soo-Youn, Glucose biosensors: an overview of use in clinical practice, Sensors 10 (2010) 4558–4576.
[2] Y. Li, X. Wu, J. Song, J. Li, Q. Shao, N. Cao, N. Lu, Z. Guo, Reparation of recycled acrylonitrile- butadiene-styrene by pyromellitic dianhydride: reparation performance evaluation and property analysis, Polymer 124 (2017) 41–47.
[3] A.L. Galant, R.C. Kaufman, J.D. Wilson, Glucose: detection and analysis, Food Chem. 188 (2015) 149–160.
[4] J.D. Newman, A.P.F. Turner, Home blood glucose biosensors: a commercial perspective, Biosens. Bioelectron. 20 (2005) 2435–2453.
[5] S.N. Thennadil, J.L. Rennert, B.J. Wenzel, K.H. Hazen, T.L. Ruchti, M.B. Block, Comparison of glucose concentration in interstitial fluid, and capillary and venous blood during rapid changes in blood glucose levels, Diabetes Technol. Ther. 3 (2001) 357.
[6] E. Cengiz, W.V. Tamborlane, A tale of two compartments: interstitial versus blood glucose monitoring, Diabetes Technol. Ther. 11 (1) (2009) S11.
[7] W. Gao, S. Emaminejad, H.Y.Y. Nyein, S. Challa, K. Chen, A. Peck, H.M. Fahad, H. Ota, H. Shiraki, D. Kiriya, D.H. Lien, G.A. Brooks, R.W. Davis, A. Javey, Fully integrated wearable sensor arrays for multiplexed in situ perspiration analysis, Nature 529 (2016) 509–514.
[8] J. Kim, S. Imani, W.R. de Araujo, J. Warchall, G. Valdes-Ramirez, T.R. Paixao, P.P. Mercier, J. Wang, Wearable salivary uric acid mouthguard biosensor with integrated wireless electronics, Biosens. Bioelectron. 74 (2015) 1061–1068.
[9] C. Liu, Y. Sheng, Y. Sun, J. Feng, S. Wang, J. Zhang, J. Xu, D. Jiang, A glucose oxidase-coupled DNAzyme sensor for glucose detection in tears and saliva, Biosens. Bioelectron. 70 (2015) 455–461.
[10] J. Kim, A.S. Campbell, J. Wang, Wearable non-invasive epidermal glucose sensors: a review, Talanta 177 (2018) 163–170.
[11] A. Soni, S.K. Jha, Smartphone based non-invasive salivary glucose biosensor, Anal. Chim. Acta 996 (2017) 54–63.
[12] J. Moyer, D. Wilson, I. Finkelshtein, B. Wong, R. Potts, Correlation between sweat glucose and blood glucose in subjects with diabetes, Diabetes Technol. Ther. 14 (2012) 398–402.
[13] K. Mitsubayashi, M. Suzuki, E. Tamiya, I. Karube, Analysis of metabolites in sweat as a measure of physical condition, Anal. Chim. Acta 289 (1994) 27–34.
[14] A. Abellan-Llobregat, I. Jeerapan, A. Bandodkar, L. Vidal, A. Canals, J. Wang, E. Morallon, A stretchable and screen-printed electrochemical sensor for glucose determination in human perspiration, Biosens. Bioelectron. 91 (2017) 885–891.
[15] A. Heller, B. Feldman, Electrochemical glucose sensors and their applications in diabetes management, Chem. Rev. 108 (2008) 2482.
[16] R. Wilson, A.P.F. Turner, Glucose oxidase: an ideal enzyme, Biosens. Bioelectron. 7 (1992) 165–185.
[17] A.A. Saei, J.E.N. Dolatabadi, P. Najafi-Marandi, A. Abhari, M. de la Guardia, Electrochemical biosensors for glucose based on metal nanoparticles, Trends Anal. Chem. 42 (2013) 216–227.
[18] H. Lee, T.K. Choi, Y.B. Lee, H.R. Cho, R. Ghaffari, L. Wang, H.J. Choi, T.D. Chung, N. Lu, T. Hyeon, S.H. Choi, D.H. Kim, A graphene-based electrochemical device with thermoresponsive microneedles for diabetes monitoring and therapy, Nat. Nanotechnol. 11 (2016) 566–572.
[19] C. Yang, M.E. Denno, P. Pyakurel, B.J. Venton, Recent trends in carbon nanomaterial-based electrochemical sensors for biomolecules: a review, Anal. Chim. Acta 887 (2015) 17–37.
[20] J. Liu, Z. Liu, C.J. Barrow, W. Yang, Molecularly engineered graphene surfaces for sensing applications: a review, Anal. Chim. Acta 859 (2015) 1–19.
[21] Y. He, X. Wang, J. Sun, S. Jiao, H. Chen, F. Gao, L. Wang, Fluorescent blood glucose monitor by hemin-functionalized graphene quantum dots based sensing system, Anal. Chim. Acta 810 (2014) 71–78.
[22] H.D. Jang, K.K. Sun, H. Chang, J.W. Choi, J. Huang, Synthesis of graphene based noble metal composites for glucose biosensor, Mater. Lett. 106 (2013) 277–280.
[23] K. Zhou, Y. Zhu, X. Yang, C. Li, Electrocatalytic oxidation of glucose by the glucose oxidase immobilized in graphene-Au-nafion biocomposite, Electroanalysis 22 (2010) 259–264.
[24] X. Wang, X. Zhang, Electrochemical co-reduction synthesis of graphene/nano-gold composites and its application to electrochemical glucose biosensor, Electrochim. Acta 112 (2013) 774–782.
[25] X. Du, Z. Zhang, Z. Miao, M. Ma, Y. Zhang, C. Zhang, W. Wang, B. Han, Q. Chen, One step electrodeposition of dendritic gold nanostructures on β-lactoglobulin-functionalized reduced graphene oxide for glucose sensing, Talanta 144 (2015) 823–829.
[26] W. He, Y. Sun, J. Xi, A.A.M. Abdurhman, J. Ren, H. Duan, Printing graphene-carbon nanotube-ionic liquid gel on graphene paper: towards flexible electrodes with efficient loading of PtAu alloy nanoparticles for electrochemical sensing of blood glucose, Anal. Chim. Acta 903 (2016) 61–68.
[27] A.K. Geim, Graphene: status and prospects, Science 324 (2009) 1530–1534.
[28] D. Chen, L. Tang, J. Li, Graphene-based materials in electrochemistry, Chem. Soc. Rev. 39 (2010) 3157–3180.
[29] H.-C. Chen, R.-Y. Tsai, Y.-H. Chen, R.-S. Lee, M.-Y. Hua, A colloidal suspension of nanostructured poly(N-butyl benzimidazole)-graphene sheets with high oxidase yield for analytical glucose and choline detections, Anal. Chim. Acta 792 (2013) 101–109.
[30] D.A. Brownson, S.A. Varey, F. Hussain, S.J. Haigh, C.E. Banks, Electrochemical properties of CVD grown pristine graphene: monolayer- vs. quasi-graphene, Nanoscale 6 (2014) 1607–1621.
[31] D.A. Brownson, C.E. Banks, The electrochemistry of CVD graphene: progress and prospects, Phys. Chem. Chem. Phys. 14 (2012) 8264–8281.
[32] X. Liang, B.A. Sperling, I. Calizo, G. Cheng, C.A. Hacker, Q. Zhang, Y. Obeng, K. Yan, H. Peng, Q. Li, X. Zhu, H. Yuan, A.R. Hight Walker, Z. Liu, L.M. Peng, C.A. Richter, Toward clean and crackless transfer of graphene, ACS Nano 5 (2011) 9144–9153.
[33] W. Zhilei, L. Zaijun, S. Xiulan, F. Yinjun, L. Junkang, Synergistic contributions of fullerene, ferrocene, chitosan and ionic liquid towards improved performance for a glucose sensor, Biosens. Bioelectron. 25 (2010) 1434–1438.
[34] J. Wang, Electrochemical glucose biosensors, Chem. Rev. 108 (2008) 814–825.
[35] A. Rabti, C.C. Mayorga-Martinez, L. Baptista-Pires, N. Raouafi, A. Merkoçi, Ferrocene-functionalized graphene electrode for biosensing applications, Anal. Chim. Acta 926 (2016) 28–35.
[36] Y. Yuan, Y. Zheng, J. Liu, H. Wang, S. Hou, Non-enzymatic amperometric hydrogen peroxide sensor using a glassy carbon electrode modified with gold nanoparticles deposited on CVD-grown graphene, Microchim. Acta 184 (2017) 4723–4729.
[37] J. Wang, Glucose biosensors: 40 Years of advances and challenges, Electroanalysis 13 (2001) 983–988.
[38] L.M. Malard, M.A. Pimenta, G. Dresselhaus, M.S. Dresselhaus, Raman spectroscopy in graphene, Phys. Rep. 473 (2009) 51–87.
[39] A.C. Ferrari, D.M. Basko, Raman spectroscopy as a versatile tool for studying the properties of graphene, Nat. Nanotechnol. 8 (2013) 235–246.
[40] P. Ilanchezhiyan, J.J. Eo, A.S. Zakirov, S.D. Gopal Ram, G.N. Panin, T.W. Kang, Au nanoparticles decorated photoresist derived multilayer graphene for transparent conducting films, Mater. Lett. 124 (2014) 18–20.
[41] A. Krajewska, K. Oberda, J. Azpeitia, A. Gutierrez, I. Pasternak, M.F. López, Z. Mierczyk, C. Munuera, W. Strupinski, Influence of Au doping on electrical properties of CVD graphene, Carbon 100 (2016) 625–631.
[42] S. Peters, S. Peredkov, M. Neeb, W. Eberhardt, M. Al-Hada, Size-dependent XPS spectra of small supported Au-clusters, Surf. Sci. 608 (2013) 129–134.
[43] Y. Zhu, S. Murali, W. Cai, X. Li, J.W. Suk, J.R. Potts, R.S. Ruoff, Graphene and graphene oxide: synthesis, properties, and applications, Adv. Mater. 22 (2010) 3906–3924.
[44] S. Sabury, S.H. Kazemi, F. Sharif, Graphene-gold nanoparticle composite: application as a good scaffold for construction of glucose oxidase biosensor, Mat. Sci. Eng. C-Mater. 9 (2015) 297–304.
[45] T.D. Thanh, J. Balamurugan, S.H. Lee, N.H. Kim, J.H. Lee, Effective seed-assisted synthesis of gold nanoparticles anchored nitrogen-doped graphene for electrochemical detection of glucose and dopamine, Biosens. Bioelectron. 81 (2016) 259–267.
[46] B. Wang, S. Yan, S. Yi, Direct electrochemical analysis of glucose oxidase on a graphene aerogel/gold nanoparticle hybrid for glucose biosensing, J. Solid State Electrochem. 19 (2015) 307–314.
[47] T.T. Baby, S.S.J. Aravind, T. Arockiadoss, R.B. Rakhi, S. Ramaprabhu, Metal decorated graphene nanosheets as immobilization matrix for amperometric glucose biosensor, Sens. Actuators B Chem. 145 (2010) 71–77.
[48] M. Mazaheri, A. Simchi, H. Aashuri, Enzymatic biosensing by covalent conjugation of enzymes to 3D-networks of graphene nanosheets on arrays of vertically aligned gold nanorods: application to voltammetric glucose sensing, Microchim. Acta 185 (2018) 178–185.

[49] A. Gutes, C. Carraro, R. Maboudian, Single-layer CVD-grown graphene decorated with metal nanoparticles as a promising biosensing platform, Biosens. Bioelectron. 33 (2012) 56–59.
[50] R. Li, J. Zhang, Z. Wang, Z. Li, J. Liu, Z. Gu, G. Wang, Novel graphene-gold nanohybrid with excellent electrocatalytic performance for the electrochemical detection of glucose, Sens. Actuators B Chem. 208 (2015) 421–428.
[51] R. Devasenathipathy, V. Mani, S.M. Chen, S.T. Huang, T.T. Huang, C.M. Lin, K.Y. Hwa, T.Y. Chen, B.J. Chen, Glucose biosensor based on glucose oxidase immobilized at gold nanoparticles decorated graphene-carbon nanotubes, Enzym. Microb. Technol. 78 (2015) 40–45.
[52] X. Xuan, H.S. Yoon, J.Y. Park, A wearable electrochemical glucose sensor based on simple and low-cost fabrication supported micro-patterned reduced graphene oxide nanocomposite electrode on flexible substrate, Biosens. Bioelectron. 109 (2018) 75–82.
[53] B. Wu, S. Hou, Y. Xue, Z. Chen, Electrodeposition-Assisted assembled multilayer films of gold nanoparticles and glucose oxidase onto polypyrrole-reduced graphene oxide matrix and their electrocatalytic activity toward glucose, Nanomaterials 8 (2018) 993–1005.
[54] Y. Chen, Y. Li, D. Sun, D. Tian, J. Zhang, J.-J. Zhu, Fabrication of gold nanoparticles on bilayer graphene for glucose electrochemical biosensing, J. Mater. Chem. 21 (2011) 7604.
[55] R.K. Shervedani, A. Amini, Novel graphene-gold hybrid nanostructures constructed via sulfur modified graphene: preparation and characterization by surface and electrochemical techniques, Electrochim. Acta 121 (2014) 376–385.
[56] Z. Pu, R. Wang, K. Xu, D. Li, H. Yu, A flexible electrochemical sensor modified by graphene and AuNPs for continuous glucose monitoring, Sensors 1 (2016) 1–6.
[57] X. Qin, W. Lu, A.M. Asiri, A.O. Al-Youbi, X. Sun, Green, low-cost synthesis of photoluminescent carbon dots by hydrothermal treatment of willow bark and their application as an effective photocatalyst for fabricating Au nanoparticles-reduced graphene oxide nanocomposites for glucose detection, Catal. Sci. Technol. 3 (2013) 1027–1035.
[58] D. Maity, M. C.R, R.K. R.T, Glucose oxidase immobilized amine terminated multiwall carbon nanotubes/reduced graphene oxide/polyaniline/gold nanoparticles modified screen-printed carbon electrode for highly sensitive amperometric glucose detection, Mater. Sci. Eng. C 105 (2019) 110075–110085.
[59] T.C. Gokoglan, M. Kesik, S. Soylemez, R. Yuksel, H.E. Unalan, L. Toppare, Paper based glucose biosensor using graphene modified with a conducting polymer and gold nanoparticles, J. Electrochem. Soc. 164 (2017) G59–G64.
[60] C. Shan, H. Yang, D. Han, Q. Zhang, A. Ivaska, L. Niu, Graphene/AuNPs/chitosan nanocomposites film for glucose biosensing, Biosens. Bioelectron. 25 (2010) 1070–1074.
[61] S.-J. Li, T.-W. Chen, N. Xia, Y.-L. Hou, J.-J. Du, L. Liu, Direct electrochemistry of glucose oxidase on sulfonated graphene/gold nanoparticle hybrid and its application to glucose biosensing, J. Solid State Electrochem. 17 (2013) 2487–2494.
[62] M.A. Akhtar, R. Batool, A. Hayat, D. Han, S. Riaz, S.U. Khan, M. Nasir, M.H. Nawaz, L. Niu, Functionalized graphene oxide bridging between enzyme and Au-sputtered screen-printed interface for glucose detection, ACS Appl. Nano Mater. 2 (2019) 1589–1596.